The following Communications have been judged by at least two referees to be "very important papers" and will be published online at www.angewandte.org soon:

*S. Arita, T. Koike, Y. Kayaki, T. Ikariya**
Aerobic Oxidative Kinetic Resolution of Racemic Secondary Alcohols with Chiral Bifunctional Amido Complexes

*T. Z. Forbes, J. G. McAlpin, R. Murphy, P. C. Burns**
Metal–Oxygen Isopolyhedra Assembled into Fullerene Topologies

T. A. Rokob, A. Hamza, A. Stirling, T. Soós, I. Pápai**
Turning Frustration into Bond Activation: A Theoretical Mechanistic Study on Heterolytic Hydrogen Splitting by Frustrated Lewis Pairs

*E. Stavitski, M. H. Kox, I. Swart, F. M. de Groot, B. M. Weckhuysen**
In Situ Synchrotron-Based IR Microspectroscopy To Study Catalytic Reactions in Zeolite Crystals

*C. Ruspic, J. R. Moss, M. Schürmann, S. Harder**
Remarkable Stability of Metallocenes with Superbulky Ligands: Spontaneous Reduction of Sm^{III} to Sm^{II}

*L. M. Fidalgo, G. Whyte, D. Bratton, C. F. Kaminski, C. Abell, W. T. S. Huck**
From Microdroplets to Microfluidics: Selective Emulsion Separation in Microfluidic Devices

News

Books

Highlights

Coordination Modes

Bowled over with success: The first π coordination to a concave surface of a buckybowl has been achieved in the binding of a $\{CpFe\}^+$ unit (Cp = cyclopentadienyl) to sumanene (see picture). This was accomplished by a solid-state approach and represents an important step toward inclusion complexes of buckybowls, fullerenes, and nanotubes.

Native Chemical Ligation

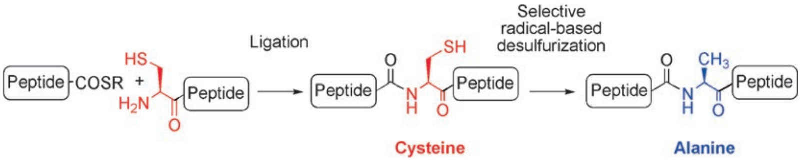

The two bottlenecks for native chemical ligation are the limitations of thioester syntheses and a lack of suitable coupling sites in peptide sequences. This Highlight describes current advances that are capable of extending the scope of these methods, such as radical desulfurization (see scheme).

Contents

Metal–Nitrogen Multiple Bonds

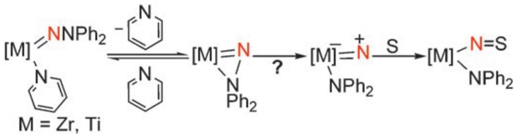

Early birds catching the worms: Early transition-metal hydrazides can now be considered to be masked metallanitrenes that are unmasked by an N—N bond activation step. Recent progress includes isolation of complexes in which migration of the group masking the metallanitrene nitrogen atom is coupled with take-up of a new substrate S (see scheme).

Reviews

Reaction Mechanisms

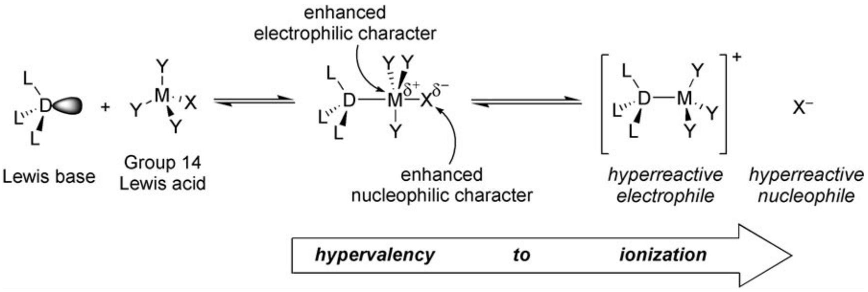

The concept of the electron pair bond by G. N. Lewis is the basis of our understanding of chemical structure and reactivity. The consequences of donor–acceptor interactions between bases and acids are manifest in the spectacular diversity of chemical transformations. A systematic analysis of the origins of these phenomena provides a unified picture of how electron-pair donors (Lewis bases) can influence chemical reactions by enhancing either (or both) electrophilic or nucleophilic character.

Communications

Microporous Materials

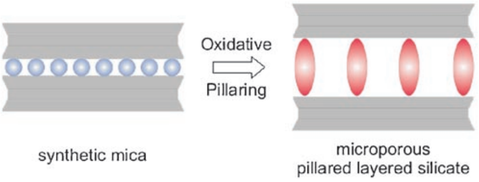

Oxidative pillaring: The intercalation of a molecular pillar (Me_2DABCO^{2+}) into synthetic Cs-tainiolite, which shows sufficient intracrystalline reactivity by an oxidative cation-exchange mechanism, yields a material with microporosity that resembles zeolites in both narrow pore size distribution and total pore volume. Owing to the high structural Fe content, this pillared clay provides a size-selective, shape-selective, and electronically conducting framework.

For the USA and Canada:
ANGEWANDTE CHEMIE International Edition (ISSN 1433-7851) is published weekly by Wiley-VCH, PO Box 191161, 69451 Weinheim, Germany. Air freight and mailing in the USA by Publications Expediting Inc., 200 Meacham Ave., Elmont, NY 11003. Periodicals postage paid at Jamaica, NY 11431. US POSTMASTER: send address changes to *Angewandte Chemie*, Wiley-VCH, 111 River Street, Hoboken, NJ 07030. Annual subscription price for institutions: US$ 7225/6568 (valid for print and electronic / print or electronic delivery); for individuals who are personal members of a national chemical society prices are available on request. Postage and handling charges included. All prices are subject to local VAT/sales tax.

Nanostructured Electrodes

Y.-S. Hu,* R. Demir-Cakan, M.-M. Titirici,* J.-O. Müller, R. Schlögl, M. Antonietti, J. Maier* ———— **1645 – 1649**

Superior Storage Performance of a Si@SiO$_x$/C Nanocomposite as Anode Material for Lithium-Ion Batteries

Full charge ahead: Hydrothermal carbonization of glucose in the presence of Si nanoparticles yields a Si@SiO$_x$/C nanocomposite that has high reversible lithium-storage capacity, excellent cycling performance, and high rate capability. This material shows promise as an anode material in lithium-ion batteries.

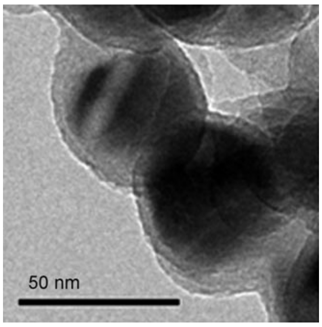

Sn–Sn Bonding

R. Jambor,* B. Kašná, K. N. Kirschner,* M. Schürmann, K. Jurkschat* ———— **1650 – 1653**

[{2,6-(Me$_2$NCH$_2$)$_2$C$_6$H$_3$}Sn]$_2$: An Intramolecularly Coordinated Diorganodistannyne

Not only steric protection by bulky substituents but also intramolecular N→Sn coordination makes possible the isolation and characterization of dimeric organotin(I) compounds such as [{2,6-(Me$_2$NCH$_2$)$_2$C$_6$H$_3$}Sn]$_2$ (see structure), which according to a crystallographic study exhibits a Sn–Sn bond length of 2.9712(12) Å.

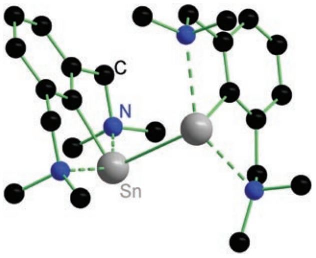

Diterpenes

J. Becker, K. Bergander, R. Fröhlich, D. Hoppe* ———— **1654 – 1657**

Asymmetric Total Synthesis and X-Ray Crystal Structure of the Cytotoxic Marine Diterpene (+)-Vigulariol

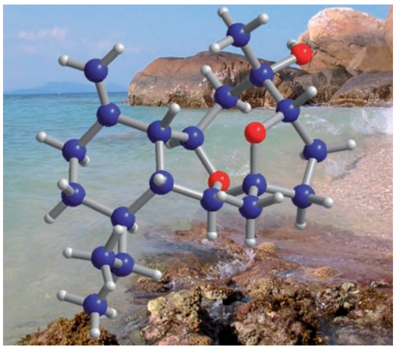

A crystal from the China sea: The asymmetric total synthesis of (+)-vigulariol (see picture: red O, blue C, white H) has been accomplished in eight linear steps starting from (*R*)-cryptone, which is readily available from eucalyptus oil. Key steps involve an asymmetric homoaldol reaction of chiral allyl carbamates and THF cyclocondensation. Ring-closing metathesis led to the tricyclic framework of the cladiellin diterpenes.

Surface Analysis

E. Bailo, V. Deckert* ———— **1658 – 1661**

Tip-Enhanced Raman Spectroscopy of Single RNA Strands: Towards a Novel Direct-Sequencing Method

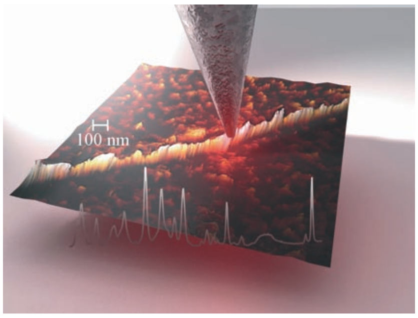

Walking the strand: Tip-enhanced Raman scattering (TERS) with precision probe positioning has been used to obtain high-quality Raman spectra of the nucleobases in a single RNA strand (see picture: foreground Raman spectrum, background atomic-force microscope tip positioned over the RNA strand). This procedure represents the first step towards direct and label-free single-biomolecule sequencing.

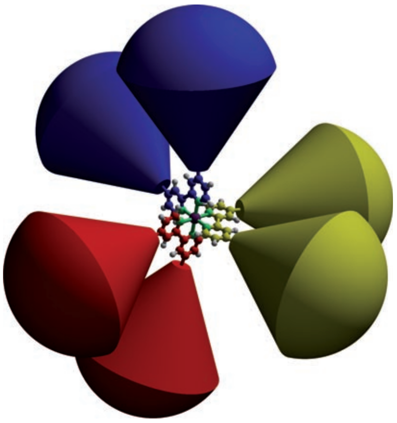

Cores for thought: Dendrimers based on an octahedral symmetry and with a central positively charged transition-metal complex have been prepared up to the third generation (see schematic representation). The shape-persistent dendrimers with a high density of aromatic rings are accessible by either a partly convergent synthesis or a divergent strategy in which the metal complex proved to be stable to high-temperature Diels–Alder reactions.

Dendrimers

M. C. Haberecht, J. M. Schnorr,
E. V. Andreitchenko, C. G. Clark, Jr.,
M. Wagner, K. Müllen* ____ **1662 – 1667**

Tris(2,2′-bipyridyl)ruthenium(II) with Branched Polyphenylene Shells: A Family of Charged Shape-Persistent Nanoparticles

---

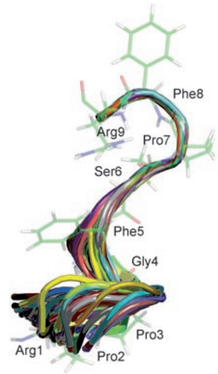

Triggering the signal: The backbone structure of the nine amino acid neuropeptide bradykinin (see picture) bound to the human G-protein coupled bradykinin subtype 2 receptor has been determined by solid-state NMR spectroscopy. Torsion-angle constraints based on ^{13}C chemical shifts were used for structure calculation, which revealed an elongated conformation with an α-helical turn at the N terminus and a β turn at the C terminus.

Protein Structures

J. J. Lopez, A. K. Shukla, C. Reinhart,
H. Schwalbe, H. Michel,
C. Glaubitz* ____ **1668 – 1671**

The Structure of the Neuropeptide Bradykinin Bound to the Human G-Protein Coupled Receptor Bradykinin B2 as Determined by Solid-State NMR Spectroscopy

---

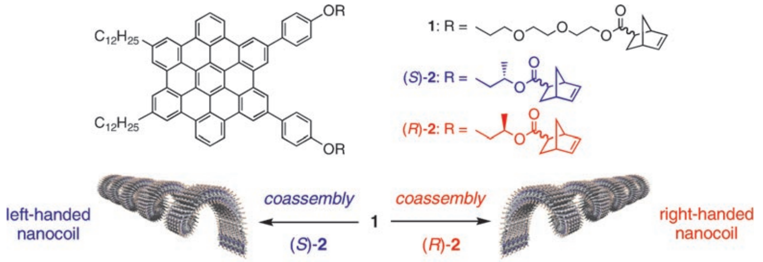

One-handed military discipline: The hexabenzocoronene (HBC) derivative **1** can coassemble with the chiral HBCs (*S*)- or (*R*)-**2** to yield graphitic nanocoils (see picture). Self-assembly of **2** alone gives noncoiled fibrous assemblies. A sergeants-and-soldiers effect leads to the formation of one-handed nanocoils. These can be covalently stabilized by post-surface ROMP of the pendant norbornene groups to give a uniform cast film. Upon doping with I_2, this film becomes electroconductive without any detectable morphological disruption.

Helical Nanocoils

T. Yamamoto, T. Fukushima,* A. Kosaka,
W. Jin, Y. Yamamoto, N. Ishii,
T. Aida* ____ **1672 – 1675**

Conductive One-Handed Nanocoils by Coassembly of Hexabenzocoronenes: Control of Morphology and Helical Chirality

Quantum Dots

R. Gill, L. Bahshi, R. Freeman,
I. Willner* ________ **1676 – 1679**

Optical Detection of Glucose and Acetylcholine Esterase Inhibitors by H_2O_2-Sensitive CdSe/ZnS Quantum Dots

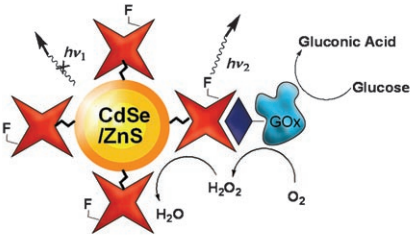

The coupling of oxidases with fluorophore-labeled CdSe/ZnS quantum dots enables the ratiometric fluorescence analysis of enzyme activities and their substrates by the interaction between the biocatalytically generated H_2O_2 and the quantum dots. The method has been applied to the analyis of glucose and the inhibition of acetylcholine esterase.

Natural Product Synthesis

E. S. Krygowski, K. Murphy-Benenato,
M. D. Shair* ________ **1680 – 1684**

Enantioselective Synthesis of the Central Ring System of Lomaivitícin A in the Form of an Unusually Stable Cyclic Hydrate

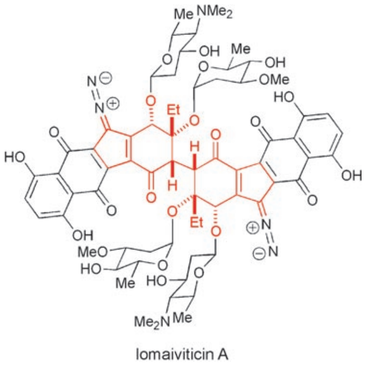

A model system representing a protected form of the four central rings of the antitumor compound lomaivitícin A has been synthesized (outlined in red in the picture). The approach features an intramolecular furan Diels–Alder reaction, a stereoselective oxidative enolate coupling to dimerize the “halves,” and a base-initiated cascade reaction. The 1,4-diketone of the central ring system exists as a stable cyclic hydrate.

Multivalent Ligands

J. Vagner, L. Xu, H. L. Handl, J. S. Josan,
D. L. Morse, E. A. Mash, R. J. Gillies,
V. J. Hruby* ________ **1685 – 1688**

Heterobivalent Ligands Crosslink Multiple Cell-Surface Receptors: The Human Melanocortin-4 and δ-Opioid Receptors

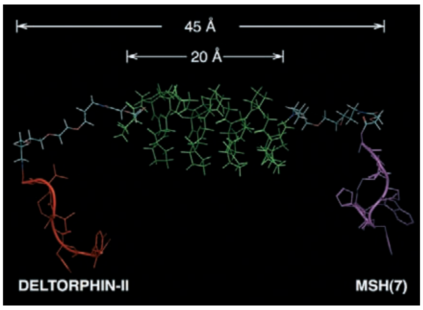

Together we bind: A series of synthetic heterobivalent ligands containing a fragment of melanocyte stimulating hormone analogue MSH(7) and the δ-opioid ligand deltorphin-II has been prepared. These ligands bind with higher affinity and with apparent cooperativity to cells expressing both hMC4R and δ-opioid receptors. Binding affinities were evaluated using a lanthanide-based in-cyto time-resolved fluorescence binding assay.

Ionic Crystals

S. Takamizawa,* T. Akatsuka,
T. Ueda ________ **1689 – 1692**

Gas-Conforming Transformability of an Ionic Single-Crystal Host Consisting of Discrete Charged Components

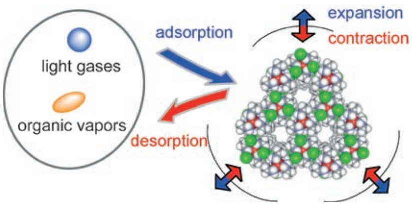

Dynamic accommodation: The racemic crystal of (±)-$[Co(en)_3]Cl_3$ (en = ethylenediamine; see space-filling model of lattice: Co red, N blue, Cl green, C gray) includes H_2O molecules within the one-dimensional channels when hydrated. Upon removal of the H_2O molecules by vacuum drying, the crystal exhibits dynamic behavior as a host to a variety of light gases or organic vapors within its channels by expansion/contraction of the lattice while single-crystal properties are maintained.

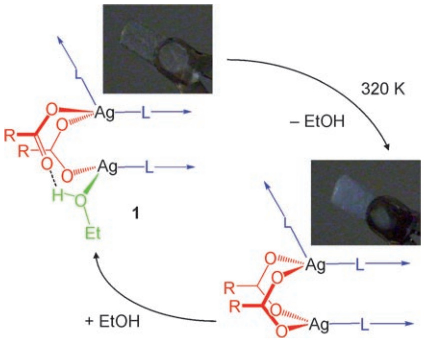

How does it fit? The one-dimensional coordination polymer $[\mathrm{Ag_4L_3\{O_2C(CF_2)_3CF_3\}_4(EtOH)_2}]_n$ (**1**; L = tetramethylpyrazine, see scheme) eliminates coordinated ethanol in an intramolecular substitution reaction. The reaction occurs in a single-crystal-to-single-crystal transformation and leads to extrusion of ethanol from the nonporous crystals. The reverse reaction involving uptake of ethanol vapor has been verified using X-ray powder diffraction.

Solid–Gas Reactions

S. Libri, M. Mahler,
G. Mínguez Espallargas,
D. C. N. G. Singh, J. Soleimannejad,
H. Adams, M. D. Burgard, N. P. Rath,
M. Brunelli, L. Brammer* ___ **1693 – 1697**

Ligand Substitution within Nonporous Crystals of a Coordination Polymer: Elimination from and Insertion into Ag–O Bonds by Alcohol Molecules in a Solid–Vapor Reaction

---

Identifying phosphatase substrates: A peptide microarray has been developed for the high-throughput study of Ser/Thr phosphatases. Putative peptide substrates, upon immobilization onto a glass slide, could be used to obtain kinetic information and identify the substrate preferences of a Ser/Thr phosphatase (see schematic representation); with this information, new biology of the enzyme could be discovered.

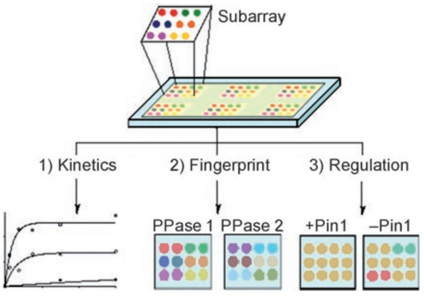

Substrate Fingerprinting

H. Sun, C. H. S. Lu, M. Uttamchandani,
Y. Xia, Y. Liou, S. Q. Yao* ___ **1698 – 1702**

Peptide Microarray for High-Throughput Determination of Phosphatase Specificity and Biology

---

Every second counts: Enhanced control over the self-organization of discotic compounds has been obtained by introducing alternating arrays of apolar (alkyl) and polar (ester) substitutents on to C_3-symmetric hexa-*peri*-hexabenzocoronenes. The local dipole moments and the nanophase separation between the polar and apolar sites significantly influence the self-assembly in solution and in the solid state (see schematic representation).

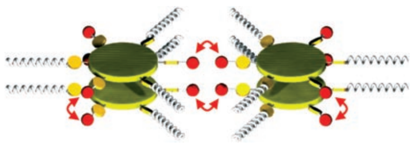

Supramolecular Chemistry

X. Feng, W. Pisula, L. Zhi, M. Takase,
K. Müllen* ___ **1703 – 1706**

Controlling the Columnar Orientation of C_3-Symmetric "Superbenzenes" through Alternating Polar/Apolar Substitutents

---

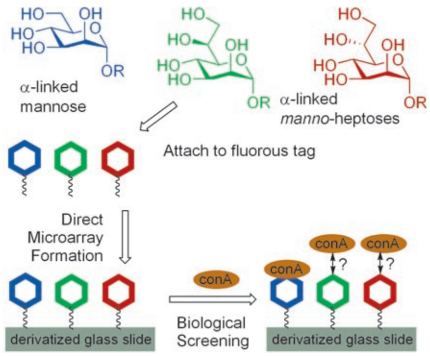

Fooling conA? Fluorous microarrays allow not only qualitative, but also quantitative assessment of binding to show that conA can accept modifications to its usual mannose ligand at the C-6 position and bind to bacterial seven-carbon mannose analogues.

Carbohydrate Microarrays

F. A. Jaipuri, B. Y. M. Collet,
N. L. Pohl* ___ **1707 – 1710**

Synthesis and Quantitative Evaluation of *Glycero*-D-*manno*-heptose Binding to Concanavalin A by Fluorous-Tag Assistance

Helical Coordination Polymers

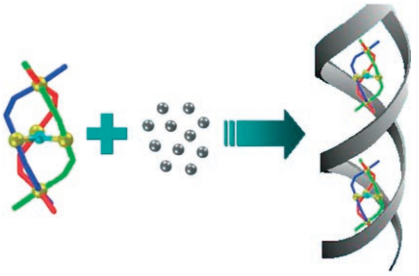

All wrapped up: Supramolecular polymeric helices were fabricated by using cluster helicates as templates. The helicity of the template (see picture; gold spheres: Ni or Zn; blue spheres: O), upon hydrothermal treatment with CuSCN (gray spheres), is transferred to the strands of the resulting copper-based coordination polymer, which is wrapped around the helicate units in the final product.

Helical Structures

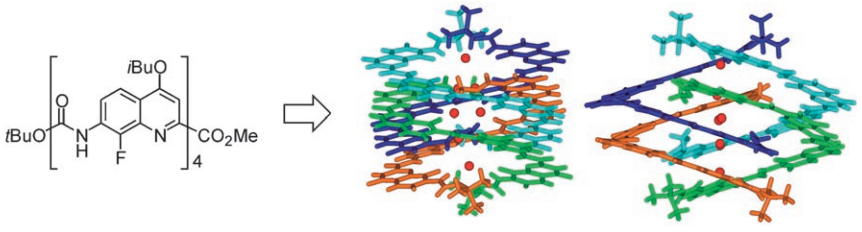

Winding and rewinding: How many times can helical aromatic oligomers wind around one another? At least four, as judged by the aggregation behavior of oligoamides based on 8-fluoroquinoline (see scheme depicting the formation of a quadruple helix; red spheres: sites in the hollow space partially occupied by water molecules).

Silyl Lewis Acids

Cationic Lewis acidic silicon species constitute a class of reactive intermediates that when “bottled” serve as useful synthetic reagents. A general way to tune the steric environment and Lewis acidic character in such species is presented.

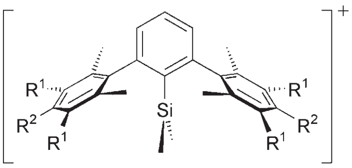

	R^1	R^2
1a	H	H
1b	H	CH_3
1c	CH_3	H
1d	CH_3	CH_3

DNA Modification

Highlighting changes in yellow: The replacement of a single oxygen atom in thymidine triphosphate with a selenium atom gave yellow 4-selenothymidine 5′-triphosphate (^{Se}TTP; see solutions of colorless natural TTP (left) and ^{Se}TTP (right)). ^{Se}TTP is recognized by DNA polymerase. Its incorporation into DNA (see scheme) yields colored DNA and occurs with the same level of efficiency as the incorporation of natural TTP.

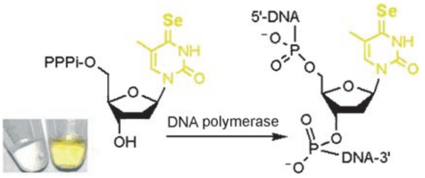

Promazine Synthesis

T. Dahl, C. W. Tornøe, B. Bang-Andersen, P. Nielsen, M. Jørgensen* **1726–1728**

Palladium-Catalyzed Three-Component Approach to Promazine with Formation of One Carbon–Sulfur and Two Carbon–Nitrogen Bonds

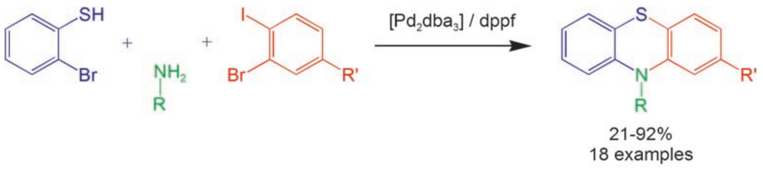

Zip it up! The use of a Pd/dppf catalyst gives access to the tricyclic phenothiazine scaffold starting from 1-bromo-2-iodobenzenes, aliphatic or aromatic amines, and 2-bromothiophenols in a single reaction flask (see scheme; dppf = 1,1′-bis(diphenylphosphanyl)ferrocene; dba = dibenzylideneacetone). This transformation involves thioether formation and subsequent intermolecular and intramolecular aryl amination reactions. The reaction occurs in good overall yield and selectivity.

Biomineralization

S. Wenzl, R. Hett, P. Richthammer, M. Sumper* **1729–1732**

Silacidins: Highly Acidic Phosphopeptides from Diatom Shells Assist in Silica Precipitation In Vitro

More decorative than wallpaper: Silica biomineralization in diatoms leads to intricate structures in the cell wall (see SEM image) and depends on structure-directing templates formed by the electrostatically driven assembly of positively charged polyamine derivatives and polyanions. The title peptides are a family of biologically relevant polyanions present in diatom biosilica and composed mainly of serine phosphate and acidic amino acid residues.

Natural Product Synthesis

M. S. Kwon, S. K. Woo, S. W. Na, E. Lee* **1733–1735**

Total Synthesis of (+)-Exiguolide

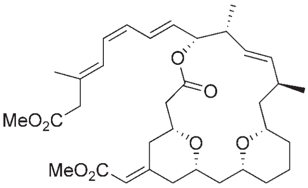

(+)-exiguolide (**1**)

The unique 16-membered macrolide (+)-exiguolide (**1**) was the target of a total synthesis featuring radical and Prins cyclizations of β-alkoxyacrylates, along with ring-closing olefin metathesis. The structure incorporates two *cis*-2,6-disubstituted oxane rings where one of the rings has an exocyclic enoate group. The successful synthesis of **1**, isolated from a marine sponge, led to the unambiguous determination of its absolute stereochemistry.

Quinine: Controversy in Synthesis

A. C. Smith, R. M. Williams* **1736–1740**

Rabe Rest in Peace: Confirmation of the Rabe–Kindler Conversion of *d*-Quinotoxine Into Quinine: Experimental Affirmation of the Woodward–Doering Formal Total Synthesis of Quinine

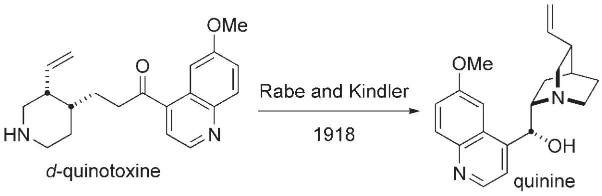

Put to rest: The three-step conversion of *d*-quinotoxine into quinine, as originally reported by Rabe and Kindler in 1918, has been experimentally verified. This conversion serves to reaffirm the formal total synthesis of quinine reported by Woodward and Doering in 1944.

Asymmetric Catalysis

K. Zhang, Q. Peng, X.-L. Hou,*
Y.-D. Wu ________ **1741 – 1744**

Highly Enantioselective Palladium-Catalyzed Alkylation of Acyclic Amides

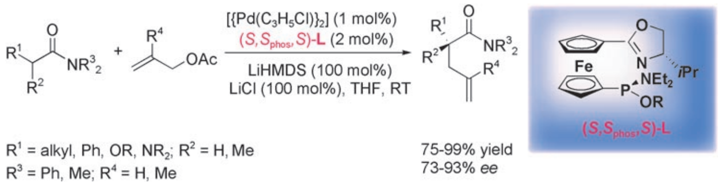

R^1 = alkyl, Ph, OR, NR$_2$; R^2 = H, Me
R^3 = Ph, Me; R^4 = H, Me

75-99% yield
73-93% *ee*

Even acyclic amides are suitable nucleophile subtrates for asymmetric allylic alkylations. The allylation products are formed in high yields in the presence of a palladium catalyst with a 1,1′-P,N ferrocene ligand (see scheme; R = (*S*)-1,1′-bi-2-naphthol). The nature of the substituents on the nitrogen atom of the amide has a critical effect on the efficiency and selectivity of the reaction.

Solvent Extraction

K. J. Bell, A. N. Westra, R. J. Warr,
J. Chartres, R. Ellis, C. C. Tong, A. J. Blake,
P. A. Tasker,* M. Schröder* . **1745 – 1748**

Outer-Sphere Coordination Chemistry: Selective Extraction and Transport of the $[PtCl_6]^{2-}$ Anion

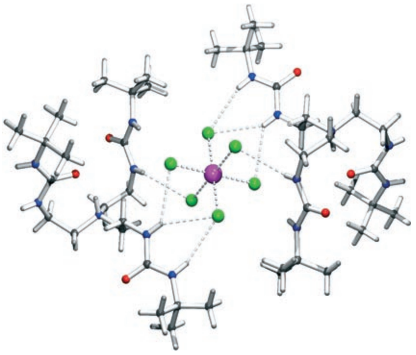

What's on the outside? Selective extraction and transport of $[PtCl_6]^{2-}$ from aqueous acidic solutions in the presence of excess chloride has been demonstrated through outer-sphere coordination of the metalloanion by tripodal polyamide and polyurea receptors (see picture; Pt purple, N blue, O red, Cl green). Loading and stripping of the organic phase can be controlled by variation of the pH value of the aqueous solution.

Nanoparticles

H.-K. Song, S. H. Lee, K. Won, J. H. Park,
J. K. Kim, H. Lee, S.-J. Moon, D. K. Kim,
C. B. Park* ________ **1749 – 1752**

Electrochemical Regeneration of NADH Enhanced by Platinum Nanoparticles

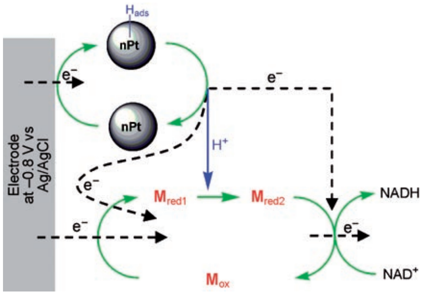

Wireless communication: Platinum nanoparticles (nPt) in an electrolyte enhance electron transfer from the electrode to NAD$^+$ during the indirect electrochemical regeneration of NADH (see picture). The intermediate nPt-H$_{ads}$, formed at negative potential, helps the turnover of the primary mediator **M** by donating a proton and an electron in a kinetically favorable way.

Catalytic DNA

P. I. Pradeepkumar, C. Höbartner,
D. A. Baum,
S. K. Silverman* ________ **1753 – 1757**

DNA-Catalyzed Formation of Nucleopeptide Linkages

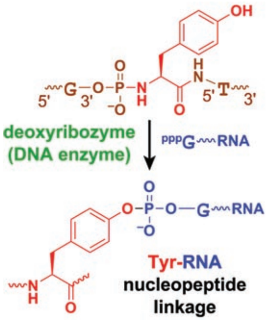

Joining amino acids and nucleotides: A deoxyribozyme catalyzes the nucleophilic attack of a tyrosine (Tyr) side chain on a 5′-triphosphate RNA, efficiently forming a Tyr–RNA nucleopeptide linkage (see picture). Thus, the scope of known DNA catalysis is further expanded beyond reactions of oligonucleotide functional groups.

Peptidic Catalysts

Z.-Z. Huang, L. J. Leman,
M. R. Ghadiri* ________ **1758 – 1761**

Biomimetic Catalysis of Diketopiperazine and Dipeptide Syntheses

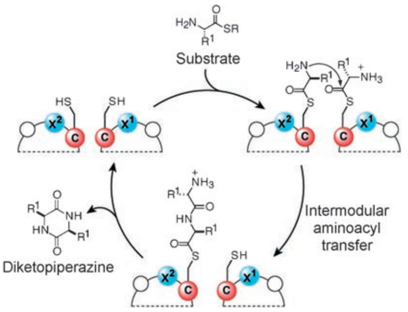

Modular supramolecular catalysts with a coiled-coil peptide scaffold, designed to mimic nonribosomal peptide synthetases, catalyze the formation of diketopiperazines and linear dipeptides for several aminoacyl substrates (see scheme). The nature of the active-site residues in the peptide catalysts can be used to effect directed intermodular aminoacyl transfer processes and govern the relative yields of diketopiperazine, linear dipeptide, and hydrolyzed substrate.

Cyanation Catalysis

C. Mazet, E. N. Jacobsen* __ **1762 – 1765**

Dinuclear {(salen)Al} Complexes Display Expanded Scope in the Conjugate Cyanation of α,β-Unsaturated Imides

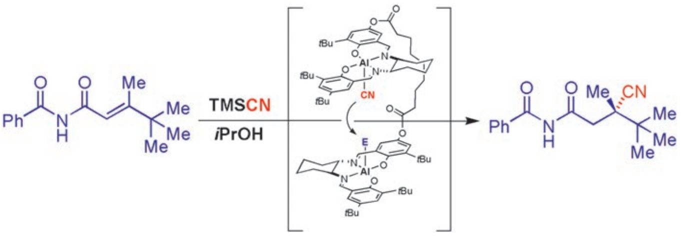

Al together: Covalently linked dinuclear {(salen)Al} complexes catalyze the conjugate cyanation of α,β-unsaturated imides with several orders of magnitude greater reactivity over the mononuclear analogue, and with comparable enantioselectivity. Imides that were completely unreactive with homo- and heterobimetallic combinations of mononuclear catalysts can now be converted into the corresponding cyanation products with high enantiomeric excess.

Surface-Phase Junctions

J. Zhang, Q. Xu, Z. Feng, M. Li,
C. Li* ________ **1766 – 1769**

Importance of the Relationship between Surface Phases and Photocatalytic Activity of TiO_2

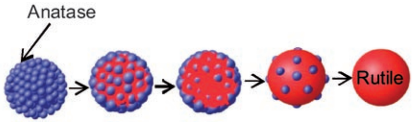

The junction boosts the function: With a combination of surface-sensitive techniques, the photocatalytic activity of TiO_2 was found to be directly related to the surface-phase structure, and can be greatly enhanced when anatase TiO_2 nanoparticles are highly dispersed on the surface of rutile TiO_2 to form anatase–rutile surface-phase junctions (see picture for calcination progression).

Asymmetric Hydrogenation

N. Arai, K. Suzuki, S. Sugizaki,
H. Sorimachi, T. Ohkuma* _ **1770 – 1773**

Asymmetric Hydrogenation of Aromatic, Aliphatic, and α,β-Unsaturated Acyl Silanes Catalyzed by Tol-binap/Pica Ruthenium(II) Complexes: Practical Synthesis of Optically Active α-Hydroxysilanes

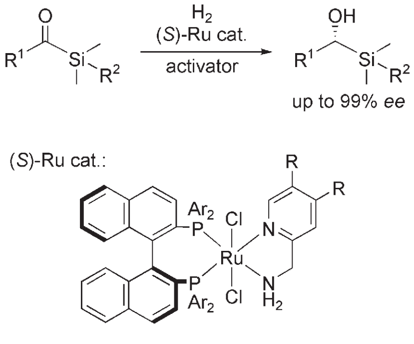

A catalytic system of Ru^{II} complex (see scheme; Ar = 4-$CH_3C_6H_4$; R = H, t-C_4H_9) and t-C_4H_9OK or $NaBH_4$ activator has been used in the hydrogenation of aromatic and aliphatic acyl silanes to give α-hydroxysilanes with high enantioselectivity (R^1 = aryl, alkyl, alkenyl; R^2 = t-C_4H_9, C_6H_5). Optically active allylic α-hydroxysilanes are obtained in the 1,2-reduction of α,β-unsaturated acyl silanes. These chiral α-hydroxysilanes are converted into 4-substituted 2-cyclopentenones without loss of enantioselectivity.

Transition-Metal Halides

A. V. Wilson, A. J. Roberts,
N. A. Young* ______ 1774 – 1776

TiF$_2$: Linear or Bent?

Calling nonlinearity into question: When Ti atoms are isolated in fluorine-doped argon matrices, TiF$_4$, TiF$_3$, TiF$_2$, and TiF are identified by their IR spectra. The Ti isotope pattern observed for the ν_3 mode of TiF$_2$ is indistinguishable from that of a linear geometry. Therefore, there is now no reliable evidence for the nonlinearity of any 3d transition-metal difluorides or dichlorides.

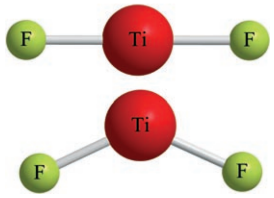

Natural Product Synthesis

M. Inoue,* I. Ohashi, T. Kawaguchi,
M. Hirama* ______ 1777 – 1779

Total Synthesis of the C-1027 Chromophore Core: Extremely Facile Enediyne Formation through SmI$_2$-Mediated 1,2-Elimination

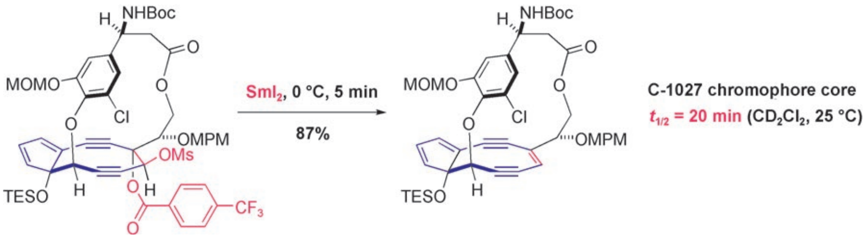

The spontaneous aromatization of the enediyne chromophore of the potent antitumor agent C-1027 generates a *p*-benzyne biradical, which cleaves double-stranded DNA. The title reaction was developed for the construction of nine-membered-ring enediynes and applied as the final step in the synthesis of the exceptionally unstable core structure of the C-1027 chromophore (see scheme; Boc, MOM, MPM, and TES are protecting groups; Ms = methanesulfonyl).

Natural Product Synthesis

K. C. Nicolaou,* G. S. Tria,
D. J. Edmonds ______ 1780 – 1783

Total Synthesis of Platencin

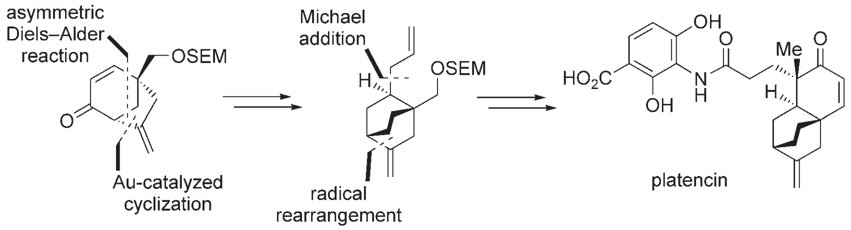

The asymmetric total synthesis of the newly discovered and potent antibiotic platencin has been achieved. The approach makes use of an asymmetric Diels–Alder reaction, a gold(I)-catalyzed cyclization, and a homoallyl radical rearrangement to forge the polycyclic architecture of this intriguing target (see scheme, SEM = 2-(trimethylsilyl)ethoxymethyl).

Supporting information is available on the WWW (see article for access details).

A video clip is available as Supporting Information on the WWW (see article for access details).

Service

Corrigendum

In Table 3 of this Communication, the chemical structures of the substituents of products **8q** and **8r** were inadvertently switched. The correct entries are shown here.

Table 3: Catalytic asymmetric hydrogenation of quinoline derivatives.[a]

Entry	R	Product	Yield [%]	*ee* [%]	Config
17	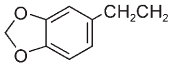	**8q**	> 99[c]	90	*R*
18	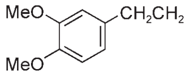	**8r**	> 99[c]	95	*R*

In Table 4, the structures of the major isomers **12a** and **12c** were printed incorrectly. The correct structures are shown here.

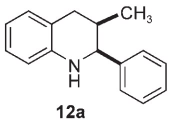

12a

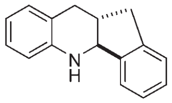

12c

The editorial office apologizes for these oversights.

The Development of Double Axially Chiral Phosphoric Acids and Their Catalytic Transfer Hydrogenation of Quinolines

Q.-S. Guo, D.-M. Du,* J. Xu ___ **759–762**

Angew. Chem. Int. Ed. **2008**, *47*

DOI 10.1002/anie.200703925